The effects of soft-segment molecular weight and organic modifier on properties of organic-modified MMT-PU nanocomposites

Chia-Hao Wang[1]*, Yeong-Tarng Shieh[2] and Steven Nutt[1]

1. Gill Foundation Composites Center, Mork Family Department of Chemical Engineering and Materials Science, University of Southern California, Los Angeles 90089-0241
2. Department of Chemical and Materials Engineering, National University of Kaohsiung, 700 Kaohsiung University Road, Nan-Tzu, Kaohsiung 811, Taiwan

Abstract: The effects of soft-segment molecular weight and organic modification of montmorillonite (MMT) on thermal and mechanical properties of segmented polyurethane (PU) elastomers were investigated. The PU/MMT nanocomposites were prepared by in situ polymerization, and the compositions included soft segments with number average molecular weights of 1000, 2000, and 2900, and organic-modified MMT (including MMT-30B and MMT-I30E). The nanocomposites produced were characterized using wide-angle X-ray diffraction (WAXD), transmission electron microscopy (TEM), Fourier transform infrared spectroscopy (FTIR), differential scanning calorimetry (DSC), and mechanical testing. The TEM and XRD results revealed that both MMT-30B and MMT-I30E were intercalated, and partially exfoliated by the PU. Mechanical tests showed that the PU1000 series in soft-segment molecular weight yielded superior tensile properties compared with the PU2000 and PU2900 series. Also, for a given molecular weight of soft segment in PU, the MMT-30B nanocomposites exhibited greater increases in Young's modulus, tensile strength, and elongation at break than the MMT-I30E counterpart, and the crystallinity of PU was enhanced by the clays.

Key words: nanoclay; fillers; nanocomposites; poly-urethanes; reinforcement

Please cite this article as C-H Wang, Y-T Shieh, and S. Nutt, "**The effects of soft-segment molecular weight and organic modifier on properties of organic-modified MMT-PU nanocomposites**", J. App. Polymers 114 (2009) 1025-1032. DOI:http://dx.doi.org/10.1002/app.30560

1. Introduction

Segmented polyurethane (PU) elastomer is a commercially important with widespread applications. Its attributes include high-abrasion resistance, shock absorption, flexibility, elasticity, and resistance to chemicals [1]. These properties originate primarily from the tendency of PU to form discrete regions of microdomains. The linear chain structure of PU can be expressed in the form of (A-B)n, where the hard segment A is composed of low-molecular weight diol or diamine (chain extender) with diisocyanate, and the soft-segment B is composed of high-molecular weight polyester or polyether polyol. Because of the different chemical structure of the hard and soft segments, repulsive interactions and thermodynamic incompatibility lead to microphase segregation [2] and formation of hard- and soft-segment domains. Moreover, the hard segments form microdomains by intermolecular hydrogen bonding in the PU [3]. Two approaches are commonly used to enhance the mechanical properties and thermal stability of PUs. The first is to alter the molecular structure of the PU (e.g., molar ratio of ingredients, molecular weight of soft segment, etc.), whereas the second approach is to introduce inorganic fillers into the PU matrix.

Organic-inorganic nanocomposites based on layered silicates were first introduced by Toyota Research Center [combining nylon and montmorillonite (MMT)] in 1993 [4–6]. Since then, the use of inorganic nanofillers in polymers has developed into the field of polymer/inorganic nanocomposites. In these materials, the introduction of small amounts of nanofillers can result in marked increases in strength, stiffness, and heat resistance compared with unreinforced (neat) polymer counterparts [7–11]. One common nanofiller is MMT clays, 2:1 layered silicates composed of two silica tetrahedral sheets and one central octahedral sheet of alumina. MMT additions can significantly improve mechanical and thermal properties for polymer/inorganic nanocomposites,

Please cite this article as C-H Wang, Y-T Shieh, and S. Nutt, "**The effects of soft-segment molecular weight and organic modifier on properties of organic-modified MMT-PU nanocomposites**", J. App. Polymers 114 (2009) 1025-1032. DOI:http://dx.doi.org/10.1002/app.30560

including polyimide, polycaprolactone, and polypropylene [12–14]. The layers are regularly stacked and bound together by weak inter-atomic forces. MMT is described by the chemical formula (Al2-yMgy)(Si4-xAlx)O10(OH)2,Mmath image in which M+ is the exchangeable cation (Na+, Ca2+, Li+), which can be substituted by an organic cation via ion exchange reaction in the galleries, and y is the degree of substitution [15].

Because of the poor compatibility of the hydrophilic inorganic silicates with hydrophobic polymer matrices, organic modification of the silicates has become the most common and efficient way to increase the hydrophobicity and thereby improve the compatibility of the composite pair. In this organic modification, the cations in the layer galleries are exchanged with cationic organic compounds (e.g., alkylammonium and alkylphosphonium). After the organic modification, the MMT not only becomes hydrophobic and thus more compatible with the polymer, but the spacing of the galleries is expanded, facilitating intercalation and/or exfoliation in polymer/MMT nanocomposites. Exfoliation of the nanoclays generally results in improved mechanical properties [16, 17].

Early work with PU/organically modified, layered silicate nanocomposites with intercalated morphology showed a large enhancement in tensile properties [18]. Similar work was followed by several studies of nanoclay composites using solution and bulk polymerization methods to intercalate the clay with soft segment polyols before reaction with isocyanates [19–25]. For example, Tien and Wei [26, 27] prepared PU/clay nanocomposites by allowing pre-polymer chain terminated with -NCO groups to react with primary ammonium modifier carrying 1–3 –CH2OH groups. They reported increases in tensile properties, glass transition temperature, and resistance to dynamic mechanical and thermal degradation with the addition of small amounts of organophilic MMT. However, the effects of the different organic modifiers and molecular weight of soft segments in

PU/clay composites on composite properties have been rarely reported. In the present study, the effects of two functionally organic-modified MMTs, MMT-30B ($Cl{-}N{+}(CH_2CH_2OH)_2(CH_3)T$ modified MMT), and MMT-I30E ($CH_3(CH_2)_{17}NH_3^+$ Cl^- modified MMT), and three molecular weights of the polyether soft segments in PU, on the properties of PU/MMT nanocomposites were investigated.

2. Experimental

2.1 Materials

The nanoclays used in the composite synthesis included two MMTs (Cloisite 30B, from Southern Clay Products, Inc, and Nanomer I.30E, from Nanocor®, Inc). Cloisite 30B is a natural MMT modified by quaternary ammonium salt. The quaternary ammonium ion has the structure, $Cl{-}N{+}(CH_2CH_2OH)_2(CH_3)T$, where T represents an alkyl group of approximately 65% $C_{18}H_{37}$, 30% C16H33, and 5%$C_{14}H_{29}$ [28]. Nanomer I.30E, however, is an octadecylammonium-modified MMT. The octadecylammonium modifier has the structure $CH_3(CH_2)_{17}NH_3^+$ Cl^-. All nanoclays were dried in a vacuum oven at 80°C for 48 h before use. After dehydration, PU was prepared using 1,4 butanediol (BDO, Avocado Research Chemicals) and polytetrahydrofuran (PTHF, Sigma-Aldrich, M.W 1000, 2000, and 2900), which are the hydroxyl-terminated monomer and oligomer, respectively. The 1,4 butanediol was dried over calcium hydride for 48 h and then was vacuum distilled. PTHF was dehydrated in a vacuum oven at 60°C for 48 h. The diisocyanate, MDI (98%, Sigma-Aldrich), was purified by filtration of molten MDI liquid at 70°C. Dimethylformamide (DMF, Sigma-Aldrich) was dehydrated and used as a solvent in the polymerization reaction.

2.2Synthesis of PU elastomer and PU/MMT nanocomposites

PU elastomer was synthesized with a molar ratio of 4 : 1 : 2.64 (MDI-to-PTHF-to-1,4BDO), using excess diisocyanate to produce partially cross-linked networks and –NCO end groups [29]. First, the oligomeric polyol (PTHF) was dissolved in DMF and reacted with MDI at 80°C for 30 min to obtain a pre-polymer in a round-bottom flask with continuous stirring under vacuum. Second, the chain extender (1,4 butanediol) was added to build up the PU network, and the mixture was allowed to react at 80°C for an additional 2 min. In initial experiments, the network building reaction was active within 2 min (after the addition of 1,4 BDO). The reaction was not completed in 2 min, but if the reaction was allowed to continue beyond 2 min, the viscosity increased rapidly, making it impossible to pour out of the round-bottom flask. Finally, the mixture was poured into a Teflon® mold and cured at 80°C for 24 h to obtain the PU elastomers. To prevent moisture absorption, the reaction was performed under vacuum and all chemicals were dehydrated beforehand.

Six batches of PU/MMT nanocomposites with different soft-segment molecular weight of PTHF (M.W 1000, 2000, and 2900) but identical nanoclay contents (2.5 wt %) were also prepared with identical molar ratios, as shown in Table I. To prepare the PU/MMT nanocomposites, two organically modified clays, including Cloisite 30B (MMT-30B) and Nanomer I.30E (MMT-I30E) were used. The polyol was dissolved in DMF and reacted with excess MDI at 80°C under vacuum for 30 min to form the pre-polymer. Next, the organically modified MMT was added to the PU pre-polymer, which was dissolved in the DMF solvent, using a high-speed dual-axis mixer (HM-500, Keyence) for 30 min. Subsequently, the chain extender 1,4 butanediol was added to the pre-polymer/MMT system and stirred vigorously for 2 min to complete the reaction. Finally, the viscous polymer was poured into a Teflon® mold and cured at 80°C for 24 h to form PU/MMT

nanocomposites. Figure 1 illustrates the steps in the synthesis route and the associated chemical structures. The samples will be referred to as PU1000 series, which includes PU1000, PU1000/MMT-30B and PU1000/MMT-I30E for soft-segment molecular weight of 1000; PU2000 series, which includes PU2000, PU2000/MMT-30B, and PU2000/MMT-I30E for soft-segment molecular weight of 2000; and PU2900 series, which includes PU2900, PU2900/MMT-30B, and PU2900/MMT-I30E for soft-segment molecular weight of 2900.

Table 1: *The composition and hard segment content of PU and PU/MMT nanocomposites*

Samples	Soft segment MW (g/mol)	PTHF (mole)	MDI (mole)	BDO (mole)	Hard segment content[a] (wt %)
PU1000	1000	1	4	2.64	55.86
PU1000/MMT-30B	1000	1	4	2.64	55.86
PU1000/MMT-I30E	1000	1	4	2.64	55.86
PU2000	2000	1	4	2.64	38.72
PU2000/MMT-30B	2000	1	4	2.64	38.72
PU2000/MMT-I30E	2000	1	4	2.64	38.72
PU2900	2900	1	4	2.64	30.00
PU2900/MMT-30B	2900	1	4	2.64	30.00
PU2900/MMT-I30E	2900	1	4	2.64	30.00

a $(W_{MDI} + W_{BDO})/(W_{PTHF} + W_{MDI} + W_{BDO})$.

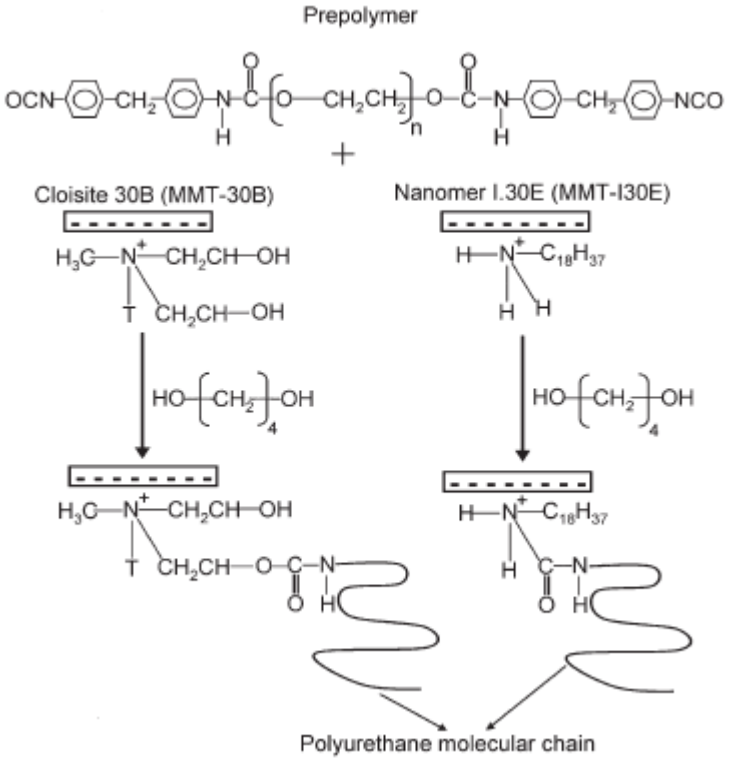

Figure 1: *Synthesis and chemical structure of PU/MMT nanocomposite.*

2.3Characterization

Wide-angle X-ray diffraction (WAXD) was performed to analyze the organic modified MMT powders (MMT-30B and MMT-I30E) and the PU/MMT nanocomposites (Bruker X-ray diffractometer, model D8 Advance). The analysis was carried out with 0.154 nm radiation, and a 2θ scan from 2.5° to 30°.

The dispersion of the MMT-30B and MMT-I30E in the PU matrix was observed using transmission electron microscopy (TEM, Philips EM420) at an acceleration voltage of 120 kV. Ultra-thin samples were sectioned by cryogenic ultra-microtoming.

IR spectroscopy was performed on the nanoclays and the nanocomposites (Nicolet 4700). For the nanoclays, KBr/MMT disks were prepared and used to obtain IR spectra for the MMT. The organically modified MMT clay (0.6 mg) and the KBr (200 mg) were mixed and pressed to make disks. The IR spectra of the MMT were obtained in transmission mode by FTIR spectroscopy (Nicolet 4700), and 128 scans were recorded with a resolution of 4 cm−1. For the PU and PU/MMT nanocomposites, IR spectra were obtained using the attenuated total reflection (ATR) technique, and 32 scans were collected at a resolution of 4 cm−1.

The glass transition temperatures of the soft-segment components in PU and PU/MMT nanocomposites were measured by differential scanning calorimetry (DSC 2920, TA Instruments). Measurements were performed by scanning twice to avoid signal noise and to erase thermal history. In the first scanning, the sample was heated to 250°C at 10°C/min, then cooled to −65°C. In the second scanning, the sample was heated to 300° at a heating rate of 10°/min. The second scanning was used to record transition temperatures.

Tensile strength, modulus, and elongation at break were measured using a universal testing machine (Instron 8531). Tests were performed on dog-bone shaped specimens using a crosshead speed of 10 mm/min at room temperature, in accordance with ASTM D 638-94b.

3. Results and Discussion

3.1 Morphologies of organic MMTs and PU/MMT nanocomposites

The WAXD patterns of MMT-30B, MMT-I30E, and PU/MMT nanocomposites are shown in Figure 2. The (001) diffraction peak of MMT-30B and MMT-I30E appear at diffraction angle $2\theta = 4.85°$ and 3.45°, respectively. Using the Bragg equation, the d001 spacing of MMT-30B was determined to be 1.82 nm, whereas d001 of MMT-I30E was 2.57 nm. Comparing the d spacings for MMT-30B and MMT-I30E, MMT-I30E showed a larger d spacing. The larger d spacing is associated with the higher cation exchange capacity for MMT-I30E. In addition, the arrangement of modifier molecules in MMT also affects the layer separation. Note that a small shoulder appears near 5° in the MMT-I30E pattern, and the small shoulder is attributed to the presence of nanoclay particles without organic modification. Also, the (001) peak for MMT-30B in the PU/MMT-30B nanocomposite pattern is not present, indicating that exfoliation of the silicate layer structure of the organo-clay has occurred in PU.

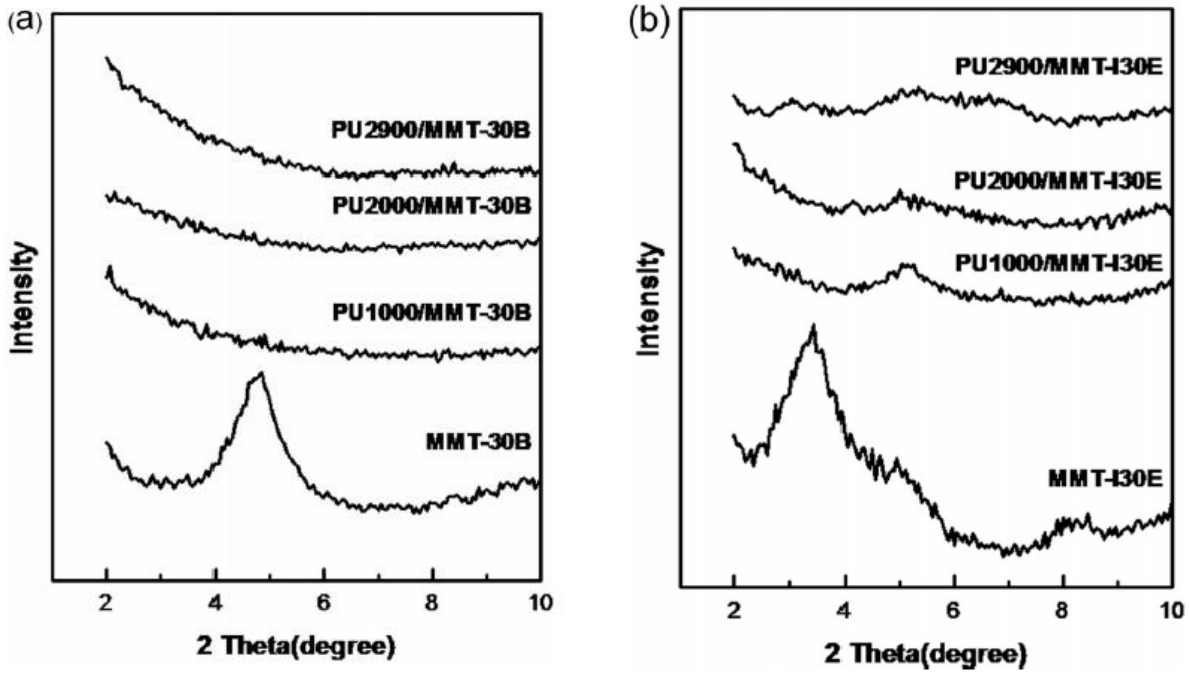

Figure 2: *WAXD patterns for (a) PU/MMT-30B and (b) PU/MMT-I30E nanocomposites.*

Similar results were obtained for the (001) peaks of PU1000/MMT-I30E and PU2000/MMT-I30E, although PU2900/MMT-I30E showed a broad hump near $2\theta = 3°$. The absence of the basal reflection in the PU1000/MMT-I30E and PU2000/MMT-I30E nanocomposites also suggests extensive exfoliation of the nano-clays in the PU matrix. However, the PU2900/MMT-I30E nanocomposite exhibited a small peak near $2\theta = 3°$, suggesting an intercalated morphology with partial exfoliation. The diffraction peak near $2\theta = 5°$ for MMT-I30 and PU/MMT-I30E nanocomposites was attributed to the incompletely modified MMT-I30E. The XRD patterns for PU/MMT-30B and PU/MMT-I30E nanocomposites may not fully reveal the levels of exfoliation or intercalation, because the concentration and order of the nano-clay can influence the XRD patterns [30]. Nevertheless, despite some limitations, the XRD results provided a useful approximation to the nanostructure from a global perspective. More detailed (and local perspective) was obtained from TEM analysis, which provided direct images of the morphology and spatial distribution of clay platelets.

Figure 3 shows TEM images of both PU2900/MMT-30B and PU2900/MMT-I30E nanocomposites with 2.5 wt % nano-clay loadings. The images show intercalated and partially exfoliated morphologies. The PU2900/MMT-30B nanocomposite, however, exhibits more extensive exfoliation than PU2900/MMT-I30E, which retains ordered layers in which the galleries are extensively expanded. From these observations of exfoliated nanoclay, the thickness of plate-like MMT-30B and MMT-I30E is ~ 1 nm, whereas the aspect ratio (length-to-thickness) is ~ 150–200 in both PU2900/MMT-30B and PU2900/MMT-I30E nanocomposites.

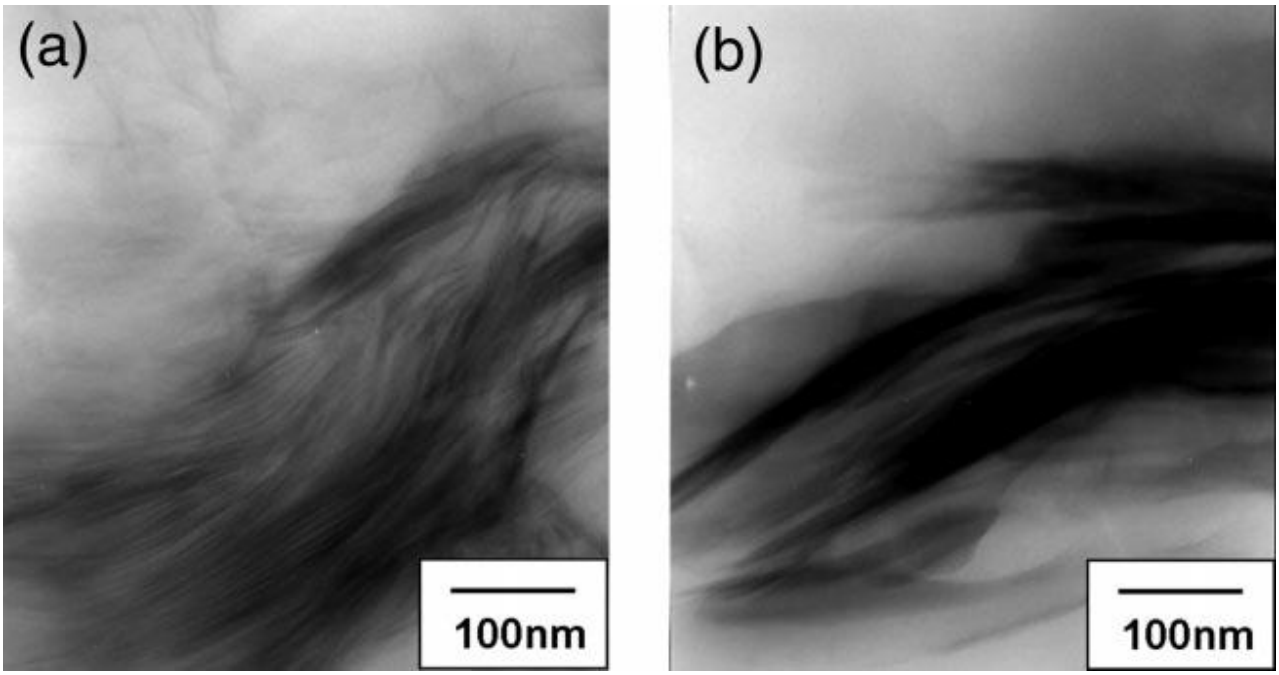

Figure 3: *TEM images of (a) PU2900/MMT-30B and (b) PU2900/MMT-I30E nanocomposites.*

The organophilic MMT had an expandable layer structure and a plate-like shape. When the chemical modifier reacted with the PU chains, the clay gallery spacings were expanded or peeled, resulting in a mixture of intercalation and partial exfoliation. This observation indicates that the MMT-30B had a stronger chemical driving force for exfoliation than the MMT-I30E when reacted with the -NCO end groups of PU. The combination of XRD patterns and morphologies observed by TEM confirm that both MMT-30B and MMT-I30E formed intercalated and partially exfoliated morphologies in PU. However, MMT-30B has two hydroxyl chain ends that are more reactive to the NCO groups of PU than MMT-I30E, in which the ammonium cation has low reactivity to the NCO groups of PU and is much less nucleophilic than the amine group. Thus, PU2900/MMT-30B exhibited more extensive exfoliation than PU2900/MMT-I30E.

3.2FTIR Characterization

The FTIR spectra of MMT-30B and MMT-I30E reveal characteristic bands of Al-OH stretching at 3627 cm−1 and a broad band of H-bonded H-O-H stretching at 3429 cm−1 (Fig. 4). The two small peaks in the spectrum of MMT-I30E near 3300 cm−1 correspond to N-H stretching vibrations, an indication that the modifier in the clay has ammonium groups. Two peaks at 2926 and 2854 cm−1 correspond to methylene groups in hydrocarbon chains of the organic ammonium ions present in both MMT-30B and MMT-I30E. The peak at 1620 cm−1 corresponds to H-O-H bending vibrations [31]. The characteristic bands of MMT at 1049, 523, and 465 cm−1 are the stretching vibration of Si-O bonds, the bending vibration of Si-O-Al, and the Si-O-Si bending vibration, respectively.

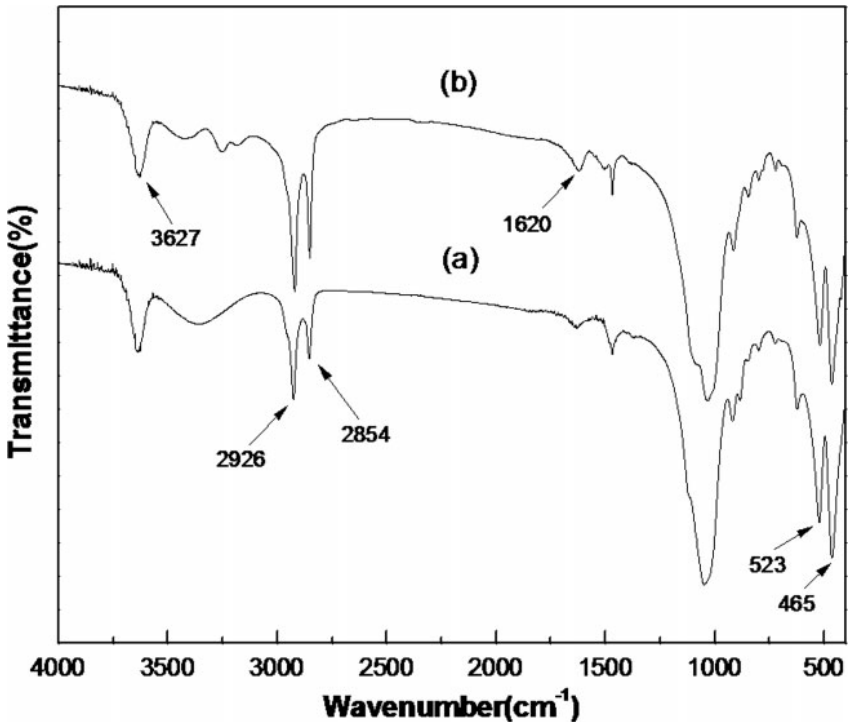

Figure 4: *FTIR spectra of (a) MMT-30B and (b) MMT-I30E.*

The FTIR spectra for PU and the PU/MMT nanocomposites are shown in Figure 5. Although the spectra are qualitatively similar, deviations in peak positions and relative peak intensities of certain bands were evident among the samples that were synthesized with identical molar ratios but with different soft-segment molecular weight and functional MMT. In particular, consider the NH and C═O stretching, which are the two most interesting regions in this study. The NH absorption peak located at 3322 cm^{-1} corresponds to hydrogen-bonded NH groups of urethane linkages [32]. This hydrogen bonding can form with hard-segment carbonyl and with soft-segment ether linkages.

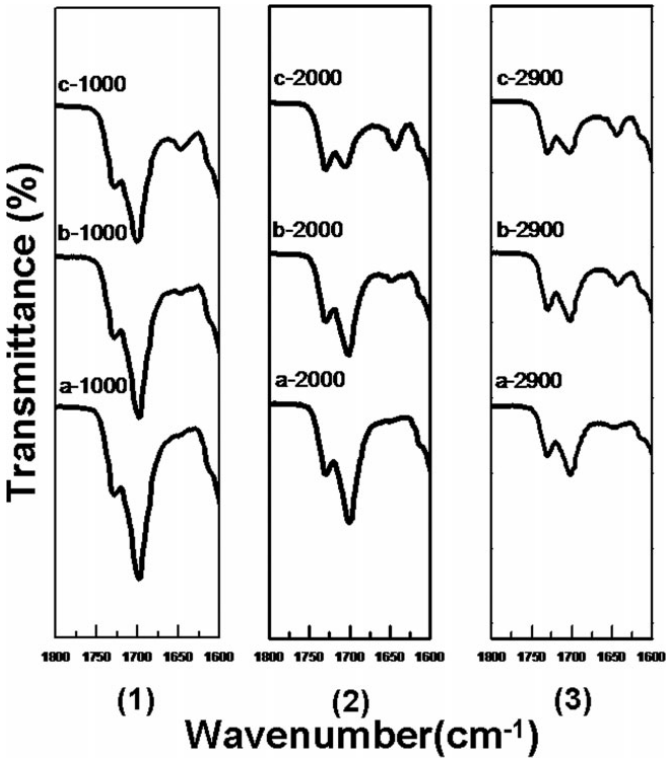

Figure 5: *FTIR spectra of (1) PU1000 series, (2) PU2000 series, and (3) PU2900 series in the range from 1650 to 1800 cm−1. (a: PU; b: PU/MMT-I30E; c: PU/MMT-30B.)*

The carbonyl bands can be divided into three regions. In Figure 5, the peak at 1729–1731 cm^{-1} is assigned to free urethane carbonyl, the peak at 1700–1704 cm^{-1} is the hydrogen-bonded urethane carbonyl, and the peak at 1643–1648 cm^{-1} is the hydrogen-bonded urea carbonyl [33]. For each

sample, the absorbencies of N—H and C═O reflect the respective concentration of these functional groups. The absence of the absorbance due to stretching of NCO groups at 2270 cm^{-1} [32] indicates that the NCO end-groups were completely reacted after the synthesis. The splitting of the carbonyl stretching absorption peak in the PU and PU/MMT nanocomposites was attributed to microphase separation on both materials [32]. Overall, the main features of the spectra for the PU/MMT nanocomposites were the same as those from the neat PU, indicating similar bond characteristics. This observation supports the conclusion that there were no major chemical structural changes in PU/MMT nanocomposites.

Peak area ratios in IR absorption spectra provided additional insights into the effects of the nano-clay additions on chemical bonding. Table II shows the peak area ratios for the free carbonyl at 1731 cm^{-1} (A_{fCO}) to the hydrogen-bonded carbonyl at 1700 cm^{-1} (A_{hCO}), and for the hydrogen-bonded NH at 3322 cm^{-1} (A_{NH}) to the CH stretching (A_{CH}) between 2811 and 2984 cm^{-1} are summarized on Table II. The value ofA_{CH} was used as an internal standard. As shown in Table II, the A_{NH}/A_{CH} ratio for each PU series was insignificantly affected by the presence of MMT. The higher A_{NH}/A_{CH} ratio for the PU series of a lower soft-segment molecular weight indicates that the content of the hard segment was greater. This observation is consistent with results shown in Table I. (This also was reflected in the tensile properties, where the PU1000 series showed greater tensile strength and modulus than the PU2000 and PU2900 series.) In addition, the A_{hCO}/A_{fCO} ratio was decreased by additions of MMT in the PU series. This result indicates that the content of the hydrogen-bonded carbonyls was decreased by MMT-30B and MMT-I30E to a greater extent than that of the free carbonyls.

Table 2: *The Area Ratio of the IR Absorption peaks of N—H Stretching (A_{NH}) and C—H Stretching (A_{CH}) and the Area Ratio of the IR Absorption Peaks of the Hydrogen-Bonded C═O (A_{hCO}) and Free C═O (A_{fCO}).*

Samples	A_{NH}/A_{CH}	A_{hCO}/A_{fCO}
PU1000	0.44	19.56
PU1000/MMT-30B	0.37	17.57
PU1000/MMT-I30E	0.37	13.23
PU2000	0.22	5.14
PU2000/MMT-30B	0.2	4.21
PU2000/MMT-I30E	0.17	1.72
PU2900	0.08	1.76
PU2900/MMT-30B	0.07	0.94
PU2900/MMT-I30E	0.11	0.6

Comparing the two nano-clays, MMT-30B had a smaller effect on the A_{hCO}/A_{fCO} ratio than MMT-30B. The smaller effect of MMT-30B is attributed to the two hydroxyl groups in the organic compound 30B that was used to modify the MMT. The more extensive hydrogen bonding between PU and the organic compound in MMT-30B was a major cause of the more extensive exfoliation in the PU/MMT-30B nanocomposite (as observed in the TEM images in Fig. 3). A second possible contributing factor is that the MMT loading (2.5 wt %) was insufficient to affect the A_{hCO}/A_{fCO} ratio in the PU/MMT nanocomposites. In related work, Pattanayak and Sadhan [34] reported that when 5 wt % MMT30B was added to PU, the hydrogen-bonded carbonyl increased. From their observations, they inferred that the urethane carbonyls reacted with residual CH_2CH_2OH groups of the quaternary ammonium ions and formed additional hydrogen bonds.

3.3Tensile Properties

The tensile yield strength (YS), Young's modulus (E), and elongation at break for PU and PU/MMT nanocomposites are presented in Table III. For a given soft-segment molecular weight, the YS, modulus, and elongation at break of PU were all increased by the clay additions, and MMT-30B resulted in a larger increase than MMT-I30E. Table III shows that the Young's modulus, tensile YS, and elongation at break of the PU2900/MMT-30B nanocomposite increased by 142%, 36%, and 49% respectively, whereas increases for the PU2900/MMT-I30E nanocomposites were more modest—21%, 9% and 11%, respectively. The PU1000 series resulted in the greatest Young's modulus and YS values among the three PU series, as expected, because of the highest hard-segment content synthesized within the PU1000 series. However, the value of elongation at break in PU1000 series is the lowest among the three PU series because of the increased hard-segment content and the associated loss of elasticity [35, 36].

Table 3: *Tensile Properties of PU and PU/MMT Nanocomposite.*

Samples	Yield strength (MPa)	Young's modulus (MPa)	Elongation at break (%)
PU1000	2.08	57.10	286
PU1000/MMT-30B	2.42	102.00	423
PU1000/MMT-I30E	2.17	59.17	338
PU2000	1.53	21.83	351
PU2000/MMT-30B	1.82	35.16	505
PU2000/MMT-I30E	1.62	23.80	393
PU2900	1.08	10.10	416
PU2900/MMT-30B	1.47	24.40	620
PU2900/MMT-I30E	1.18	12.21	462

The finding that, for a given molecular weight of soft segment, MMT-30B resulted in greater increases in YS and E than MMT-I30E is explained by the stronger interactions and higher reactivity of the two hydroxyl chain ends (MMT-30B) with the NCO groups of PU than the ammonium cation (MMT-I30E) to the NCO groups of PU. In addition, because of the large specific surface area of organophilic MMT, a large interface zone between MMT particles and PU matrix was created in both PU/MMT-30B and PU/MMT-I30E nanocomposites. As a result, when load was applied to the PU/MMT-30B and PU/MMT-I30E nanocomposites, it was transferred effectively from the matrix to the nearby nanoclay particles [37]. In this way, the load was transferred efficiently via the large interface zone for PU/MMT-30B and PU/MMT-I30E nanocomposites and the tensile properties increased substantially.

From the TEM observations (Fig. 3), the PU/MMT-30B nanocomposites were more exfoliated than the PU/MMT-I30E nanocomposites. The greater extent of exfoliation created a larger, thicker interface zone. Brinson and coworkers [38] have argued that this interface zone is effectively hardened relative to the neat polymer. To summarize, these results illustrate that uniform dispersion of the clay particles into the polymer matrix is necessary but not sufficient to enhance mechanical properties, and that surface or chemical modifications that lead to an improved interfacial adhesion between filler and matrix are also necessary.

3.4DSC Measurements

The DSC results for neat PU and PU/MMT nanocomposites with different soft-segment molecular weights are summarized in Table IV. Because the structure of PU includes hard and soft segments, two melting temperatures are expected. However, the DSC curve (not shown) revealed only one

peak, and this was associated with the melting temperature of the soft segment (T_m, SS). The peak associated with the melting temperature of the hard segment (T_m, HS) was absent from the DSC curve [39–41]. The absence was attributed to the inactive movement of hard segment, which has a small ΔCp, [42] and to the widely dispersed HS microdomains within the PU matrix [43].

Table 4: *Melting Temperature and Enthalpy of Soft Segment in PU and PU/MMT Nanocomposites.*

Samples	T_m**, SS (°C)**	ΔH **(J/g)**
PU1000	N/A	N/A
PU1000/MMT-30B	N/A	N/A
PU1000/MMT-I30E	N/A	N/A
PU2000	16.13	12.97
PU2000/MMT-30B	19.82	37.13
PU2000/MMT-I30E	20.58	27.57
PU2900	25.93	32.75
PU2900/MMT-30B	31.72	55.10
PU2900/MMT-I30E	31.92	44.79

The melting temperatures for the PU2000 and PU2900 series in the region between 16 and 32°C (Table IV) are characteristic of ordered soft-segment structures. The values also indicate that PTHF crystallized in both neat PU and PU/MMT nanocomposites with soft-segment (SS) molecular weights (MW) of 2000 and 2900. For these SS MWs, the enthalpy changes of PU2000 were increased in the presence of MMT-30B and MMT-I30E by about 24.2 and 14.6 J/g, respectively. A similar trend also occurred in the PU2900/MMT-30B and PU2900/MMT-I30E nanocomposites, which showed increases of 22.4 and 12 J/g, respectively. These increases in melting temperature and SS enthalpy in PU2000 and PU2900 were attributed to the enhancement of crystallinity by the clays

acting as nucleating agents [44]. However, in the PU1000 series, no SS melting transition (T_m, SS) was detected. This phenomenon indicated that the SS in the PU1000 series did not crystallize because of insufficient SS content. As shown in Table IV, the magnitude of the enthalpy change increased with increasing molecular weight of the soft segment for both PU2000 and PU2900 series. This result indicates that the degree of SS crystallinity is greater for the high MW SS, i.e., a higher content of the soft segment in the PU.

Korley et al [45] reported that the presence of crystallites within the soft segment could absorb strain energy during deformation. Thus, semicrystalline soft segments would act as a load-bearing phase during deformation. As shown by the DSC measurements, the MMT-30B, and MMT-I30E acted as nucleation seeds, increasing the degree of crystallinity of the soft segment. In addition, the rigid crystalline MMT clay also contributed to the increased hardness by virtue of simple reinforcement. As a result, the PU/MMT-30B and PU/MMT-I30E nanocomposites exhibited greater tensile strength and modulus values than neat PU because of the crystallization induced by the MMT clay.

Comparing the enthalpy changes in PU/MMT nanocomposites with similar SS MWs, the PU/MMT-30B nanocomposites exhibited greater crystallinity than the PU/MMT-I30E nanocomposites in the PU2900 and PU2000 series. The greater crystallinity can be explained by the fact that the —CH_2CH_2OH groups attached to the MMT-30B had stronger interactions and higher reactivity with PU than the —NH groups in MMT-I30E. Although the —CH_2CH_2OH groups reacted with hard segments in the PU, the hard segment mobility was restricted by the MMT-30B clay. In contrast, the soft segments had greater mobility and free volume to produce greater crystallization for the PU/MMT-30B nanocomposites. However, as discussed previously, the soft segments in the PU1000 series did not crystallize, yet resulted in superior tensile properties relative to the PU2000 and

PU2900 series because of the highest hard-segment content synthesized within the PU1000 series. This supports the assertion that the hard segment concentration affected the tensile properties more strongly than the degree of SS crystallinity for the PU1000 series.

4. Conclusions

PU/MMT nanocomposites were prepared by *in-situ* polymerization reactions. The resulting nanocomposites exhibited increases in degree of crystallinity and mechanical strength compared with the neat PU. These findings were attributed to the chemical modification of MMT, especially for —CH_2CH_2OH groups on MMT-30B nanoclay, which led to stronger interactions and reactivity with the matrix system. In particular, the modifications led to strong chemical bonding between the dispersed and continuous phases, as well as intercalation and partial exfoliation of the nanoclays, both of which contributed to the enhancement in strength, modulus, and elongation at break. Generally, the effect of different SS MWs on the mechanical and thermal properties of PU/MMT nanocomposites resembled the tendencies observed for neat PU. That is, as the SS MW was increased, the tensile strength and modulus decreased for both the neat PU and the PU/MMT nanocomposites. However, the WAXD data pattern indicated that when the SS MW was increased in the nanocomposites (particularly PU2900/MMT-I30E), the increase in tangled SS molecular chains altered the morphology of the MMT in PU/MMT nanocomposites, reducing the interaction between nanoclays and the soft segments. Thus, while the two approaches—varying SS MWs and adding modified nanoclay—can be combined, interference can occur in some circumstances, diminishing the beneficial effects. This finding highlights the complexity of designing nanocomposites which combine strengthening approaches. Nevertheless, the findings indicate that

suitable modification of nanoclays and judicious selection of SS MW of components can be combined to achieve additive effects, further expanding the design space for nanocomposites.

References

1. Fakirov, Stoyko. Handbook of Condensation Thermoplastic Elastomers; Wiley-VCH, Germany, 2006; p 643. ISBN: 9783527606610.
2. Lin, J. R.; Chen, L. W. J Appl Polym Sci 1998, **69**, 1563.
3. Penczek, P.; Frisch, K. C.; Szczepaniak, B.; Rudnik, E. J Polym Sci Chem 1993, **31**, 1211.
4. Kojima, Y.; Usuki, A.; Kawasumi, M.; Okada, A.; Kurauchi, T.; Kamigaito, O. J Polym Sci Polym Chem 1993, **31**, 983.
5. Kojima, Y.; Usuki, A.; Kawasumi, M.; Okada, A.; Kurauchi, T.; Kamigaito, O.; Kaji, K. J Polym Sci Polym Phys 1994, **32**, 625.
6. Kojima, Y.; Usuki, A.; Kawasumi, M.; Okada, A.; Kurauchi, T.; Kamigaito, O.; Kaji, K. J Polym Sci Polym Phys 1995, **33**, 1039.
7. Wang, Ke; Chen, Ling; Kotaki, Masaya; He, Chaobin. Compos Appl Sci Manuf 2007, **38**, 192.
8. Qi, B.; Zhang, Q. X.; Bannister, M.; Mai, Y. W. Compos Struct 2006, **75**, 514.
9. Ni, Ping; Li, Jing; Suo, Jishuan; Li, Shuben J Mater Sci 2004, **39**, 4671.
10. Yudina, V. E.; Otaigbeb, J. U.; Gladchenkoa, S.; Olsonb, B. G.; Nazarenkob, S. E.; Korytkovac, N.; Gusarovc, V. V. Polymer 2007, **48**, 130.
11. Vega Baudrit, Jose; Sibaja Ballestero, Maria; Vazquez, Patricia; Torregrosa Macia, Rosa; Martın Martınez, Jose Miguel Int J Adhes Adhes 2007, **27**, 469.
12. Tyan, H. L.; Leu, C. M.; Wei, K. H. Chem Mater 2001, 13, 222.
13. Messersmith, P. B.; Giannelis, E. P. J Polym Sci Part A Polym Chem 1995, **33**, 1047.
14. Mittal, V. Eur Polym J 2007, **43**, 3727.
15. Pinnavaia, T. J. Science 1983, **220**, 365.
16. Pospiech, Doris; Kretzschmar, Bernd; Willeke, Meike; Leuteritz, Andreas; Jehnichen, Dieter; Janke, Andreas; Omastova, Maria. Polym Eng Sci 2007, **47**, 1262.
17. Wang, Jin-Cheng; Chen, Yue-Hui; Chen, Ren-Jie J Polym Sci Part B Polym Phys 2007, **45**, 519.
18. Wang, Z.; Pinnavaia, T. J. Chem Mater 1998, **10**, 3769.
19. Zilg, C.; Thomann, R.; Muelhaupt, R.; Finter, J. Adv Mater 1999, **11**, 49.
20. Petrovic, Z. S.; Javni, I.; Waddon, A.; Banhegyi, G. J Appl Polym Sci 2000, **76**, 133.
21. Tien, Y. I.; Wei, K. H. Polymer 2001, **42**, 3213.
22. Yao, K. J.; Song, M.; Hourston, D. J.; Luo, D. Z. Polymer 2002, **43**, 1017.
23. Mishra, J. K.; Kim, I.; Ha, C. S. Macromol Rapid Commun 2003, **24**, 671.
24. Song, M.; Hourston, D. J.; Yao, K. J.; Tay, J. K. H.; Ansarifar, M. A. J Appl Polym Sci 2003, **90**, 3239.
25. Rhoney, I.; Brown, S.; Hudson, N. E.; Pethrik, R. A. J Appl Polym Sci 2003, **91**, 1335.
26. Tien, Y. I.; Wei, K. H. Macromolecules 2001, **34**, 9045.
27. Tien, Y. I.; Wei, K. H. J Appl Polym Sci 2002, **86**, 1741.
28. http://www.nanoclay.com/data/30B.htm.
29. Prisacariu, C.; Olley, R. H.; Caraculacu, A. A.; Bassett, D. C.; Martin, C. Polymer 2003, **44**, 5407.
30. Morgan, A. B.; Gilman, J. W. J Appl Polym Sci 2002, **87**, 1329.
31. Madejova´ , J. Vib Spectrosc 2003, **31**, 1.
32. Pattanayak, Asim; Jana, Sadhan C. Polymer 2005, **46**, 5183.
33. Wang, Carl B.; Cooper, Stuart L. Macromolecules 1983, **16**, 775.
34. Pattanayak, Asim; Jana, Sadhan C. Polymer 2005, **46**, 3394.

Please cite this article as C-H Wang, Y-T Shieh, and S. Nutt, "**The effects of soft-segment molecular weight and organic modifier on properties of organic-modified MMT-PU nanocomposites**", J. App. Polymers 114 (2009) 1025-1032. DOI:http://dx.doi.org/10.1002/app.30560

35. Nielsen, L. E. Rheol Acta 1974, **13**, 86.
36. Treloar, L. R. G. The Physics of Rubber Elasticity, 3rd ed.; Clarendon Press: Oxford, 1975.
37. Tsai, Jialin; Sun, C. T. J Compos Mater 2004, **38**, 567.
38. Etan, A.; Fisher, F. T.; Andrews, R.; Brinson, L. C.; Schadler, L.
39. S. Compos Sci Technol 2006, **66**, 1159.
40. Speckhard, T. A.; Hwang, K. K. S.; Yang, C. Z.; Laupan, W. R.; Cooper, S. L. J Macromol Sci Phys B 1984, **23**, 175.
41. Macknight, W. J.; Yang, M.; Kajiyama, T. Polym Prepr (Am Chem Soc Div Polym Chem) 1968, **9**, 860.
42. Yang, C. Z.; Hwang, K. K. S.; Cooper, S. L. Makromol Chem 1983, **184**, 651.
43. Yilgor, I.; Riffle, J. S.; Wilkes, G. L.; Mcgrath, J. E. Polym Bull 1982, 8535.
44. Li, Y.; Tong, G.; Liu, J.; Linliu, K.; Desper, C. R.; Chu, B. Macromolecules 1992, **25**, 7365.
45. Sun, Li; Yang, Jin-Tao; Lin, Gen-Yao; Zhong, Ming-Qiang. Mater Lett 2007, **61**, 3963.
46. Korley, James; Lashanda, T.; Pate, Brian D.; Thomas, Edwin L.; Hammond, Paula T. Polymer 2006, 47, 3073.Sci Chem 1993, **31**, 1211.